Tuning the rheological properties of laccase-crosslinked arabinoxylan hydrogels by prior arabinofuranosidase treatments

Food Hydrocolloids 172 (2026) 112080

Contents lists available at ScienceDirect

Food Hydrocolloids

journal homepage: www.elsevier.com/locate/foodhyd

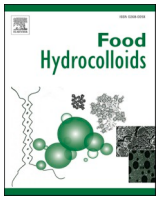

Tuning the rheological properties of laccase-crosslinked arabinoxylan hydrogels by prior arabinofuranosidase treatments

Carl Rämgård [a], Marjorie Ladd Parada [a], Ratchawit Janewithayapun [b], Thu V. Vuong [c], Emma R. Master [c], Anna Ström [b], Lauren S. McKee [a], Francisco Vilaplana [a,*]

[a] Division of Glycoscience, Department of Chemistry, School of Engineering Sciences in Chemistry, Biotechnology and Health, KTH Royal Institute of Technology, AlbaNova University Centre, SE-106 91, Stockholm, Sweden
[b] Department of Chemistry and Chemical Engineering, Division of Applied Chemistry, Chalmers University of Technology, Göteborg, SE, 41296, Sweden
[c] Department of Chemical Engineering and Applied Chemistry, University of Toronto, 200 College Street, Toronto, Ontario, M5S 3E5, Canada

ARTICLE INFO

Keywords:
Arabinoxylan
Hydrogels
Crosslinking
Enzyme technology
Rheological properties

ABSTRACT

Arabinoxylans are the most abundant polysaccharides in the bran from wheat and rye kernels. Ferulic acid moieties covalently bound to arabinosyl substitutions in arabinoxylans can be oxidised and crosslinked by laccase enzymes, forming xylan hydrogels stabilised by chemical and physical interactions. Here, we explore the use of α-L-arabinofuranosidases to tune the rheological properties of laccase-crosslinked feruloylated arabinoxylans from wheat (WAX) and rye (RAX) brans, proposed to be mediated via intermolecular backbone interactions. The effect of subsequent freeze-drying and regeneration of the hydrogels on their multiscale structure and viscoelastic properties was further evaluated by X-ray scattering, microscopy and rheology measurements. The combined use of α-L-arabinofuranosidases from glycosyl hydrolase (GH) families GH62 and GH43 with complementary specificity towards different substitution motifs in arabinoxylan resulted in synergistic arabinose removal with a 48 % and 33 % increase in arabinose removal in WAX and RAX respectively, while retaining the ferulic acid moieties in both WAX and RAX. The extent of ferulic acid oxidation in WAX and RAX seemed to be affected by substrate inaccessibility for the laccase and polysaccharide chain aggregation, which was further accentuated by enzymatic arabinose removal. Rheological investigations revealed that laccase-crosslinked WAX hydrogels pretreated with arabinofuranosidases showed a decrease of 65–95 % in the storage and loss moduli compared to the non-pretreated WAX hydrogels, whereas arabinose removal improved the viscoelastic properties of RAX hydrogels both before and after regeneration, with an increase of storage moduli of 72–100 %. Arabinofuranosidase treatments and freeze-drying/regeneration altered the hydration properties of the hydrogels and their network structure, promoting the occurrence of ordered domains. Our results show that the biophysical properties of the arabinoxylans in terms of aggregation and hydration largely influence substrate accessibility to laccase-mediated oxidation and the multiscale assembly of the hydrogels upon freeze drying and regeneration, thus impacting their overall rheological properties. These dietary fibre hydrogels from cereal side streams have large potential to be used as food hydrocolloids, contributing to the overall circularity of the food system.

1. Introduction

Despite ongoing efforts in developing industrial processes and public awareness, food losses increase every year (Gustavsson et al., 2011), which account for a total yearly economic loss value of over USD $900 Billion (FAO, 2014). In the European Union, the manufacturing of food products from agricultural industries contributes almost 22 % of total food loss (EUROSTAT, 2021). One major side stream product from agricultural processing is bran, present in most common cereal grains. For wheat, bran makes up 14–25 % of the total grain weight (Amritpal et al., 2019; Neves et al., 2006). Bran is typically removed from the harvested wheat to produce white flour instead of using the whole grain, due to consumer demands relating to taste and texture profiles of cereal-based products. Only 10 % of wheat bran produced is utilised in baked goods or as dietary supplements, despite its positive nutritional profile (Rahman et al., 2017). While there are other uses for this

* Corresponding author.
E-mail address: franvila@kth.se (F. Vilaplana).

https://doi.org/10.1016/j.foodhyd.2025.112080
Received 31 July 2025; Received in revised form 3 October 2025; Accepted 4 October 2025
Available online 5 October 2025

agricultural byproduct, such as animal feed, large fractions unfortunately remain unused in the mills (Cui et al., 2013). As such, the abundantly available and under-used bran of many cereal grains is a potentially important raw material for valorisation into food products for human consumption.

Bran is the outer fibrous tissue (pericarp and aleurone) surrounding the endosperm of cereal grains, providing protection and mechanical support to the starchy endosperm (Fig. 1A). The bran is chiefly composed of a variety of indigestible polysaccharides (dietary fibres), the most abundant being arabinoxylan (Luc et al., 2007). Arabinoxylans are composed of a (1 → 4)-linked β-D-xylopyranose (Xyl*p*) backbone, which itself is substituted by α-(1 → 2)- and/or α-(1 → 3)-linked L-arabinofuranosyl (Ara*f*) residues (Nyström et al., 2008). Arabinoxylan has prebiotic features (Broekaert et al., 2010; Rosicka-Kaczmarek et al., 2016) and can be utilised to improve the rheological properties in dough (Amritpal et al., 2019). In addition to the glycan components, bran also has a significant phenolic content in the native cell wall, with the most abundant phenolic moiety being ferulic acid. Ferulic acid is covalently attached to the arabinoxylan core, esterified to the arabinosyl substitutions usually at the *O*-5 position (Fig. 1B) (Hatfield et al., 1999). Wheat and rye brans are both good sources of ferulic acid (Aura, 2014), which along with other phenolic compounds, has been shown to work as a radical scavenger, and thus provide antioxidant benefits (Mendis & Simsek, 2014). Arabinoxylan can be extracted from bran using alkaline extraction (Aguedo et al., 2014). However, the alkaline conditions used in typical extraction processes remove most phenolic groups through saponification, leading to the loss of ferulic acid and its beneficial antioxidant behaviour (Ruthes et al., 2017). Instead, using subcritical water extraction arabinoxylan can be readily extracted from bran in polymeric form while retaining the phenolic substitutions in high amounts covalently bound to the arabinoxylans. (Rudjito et al., 2020; Ruthes et al., 2017; Yilmaz-Turan, Jiménez-Quero, Moriana, et al., 2020). The extracts have radical scavenging properties, due to the presence of bound ferulic acid (Yilmaz-Turan, Jiménez-Quero, Menzel, et al., 2020).

From a structural perspective, ferulic acid also has the potential to undergo oxidative crosslinking between different units and form dimeric ferulic acid bridges between the arabinoxylan chains, or dehydrodimeric ferulic acids (Di-FAs) (Geissmann & Neukom, 1973). These crosslinking dimers can occur naturally within the cell walls of wheat and rye due to the action of the plants' own peroxidase enzymes (Fry et al., 2000). In recent years, it has been shown that ferulic acid can also be crosslinked into dimers using laccase enzymes from fungi (Abdulhadi et al., 2014; Ikehata et al., 2004; Oluyemisi et al., 2012). Laccases, more commonly associated with lignin degradation, oxidise the hydroxyl groups on ferulic acids, which in turn create a radical that can through resonance stabilisation occupy different positions on the benzene ring in ferulic acid (Kudanga et al., 2011). This radical can be stabilised by coupling with another radical from a different oxidised ferulic acid to create a covalently linked dimer (Fig. 1C) (Adelakun et al., 2012; Carunchio et al., 2001). Because of the variability of radical positioning, different types of Di-FAs can be created, such as 5-5′, 8-8′, 8-5' cyclic/non-cyclic, and 8-O-4- isomers (Abdulhadi et al., 2014; Garcia-Conesa et al., 1997; Oluyemisi et al., 2012). Because of this crosslinking, extracted arabinoxylans can form a 3-dimensional hydrogel network thus creating a hydrogel using edible compounds of high prebiotic value (Carvajal-Millan et al., 2005).

While the main driving force behind the gelation of arabinoxylan is the chemical crosslinking of ferulic acid, there are other factors that can affect the structural and rheological properties of the hydrogels. Physical interactions by hydrogen bonding and non-polar interactions between the arabinoxylans are suspected to strengthen hydrogels (Vansteenkiste et al., 2004), and previous work has shown that freeze drying hydrogels then regenerating them in water improves their rheological properties (Yilmaz-Turan et al., 2022), possibly due to an increased interaction between the xylan backbone or due to an increase in total solid content in the hydrogels. The degree of substitution of arabinoxylan also affects the hydrogel's rheological properties (Marquez-Escalante et al., 2018), possibly due to the occurrence of intermolecular interactions between the exposed xylan backbones. In this context, the use of xylan-debranching arabinofuranosidase enzymes catalysing the hydrolytic cleavage of arabinose substitutions from the xylan backbone has potential to modulate the physico-chemical properties of arabinoxylans (Höije et al., 2008; Selig et al., 2015; Vuong & Master, 2022). Arabinofuranosidases are glycosyl hydrolases (GH) that are usually found in families GH43, GH51, GH54, and GH62 (Vuong et al., 2024), with distinct activity and selectivity towards terminal arabinose units in arabinoxylans depending on their glycosidic linkage, structural context (i.e. single versus double substitution), and the polysaccharide's molar mass.

This study aims to tailor the rheological properties of arabinoxylan hydrogels using enzyme technology, combining arabinofuranosidase-mediated xylan debranching and laccase oxidation of the resulting polysaccharides to control the occurrence of chemical crosslinks and physical chain interactions in the arabinoxylan hydrogel network. This is achieved by investigating which variables may be the driving forces behind the gelation of arabinoxylan hydrogels and how these variables impact the hydrogels' functional properties. We studied the effect of selective enzymatic hydrolysis by arabinofuranosidases from families GH43 and GH62 to modify the degree of substitution of arabinoxylans extracted from wheat and rye bran, and the subsequent effect of arabinoxylan debranching on the formation of Di-FA dimers through laccase-mediated oxidation. After laccase-induced crosslinking of the modified arabinoxylan, we evaluated the effect of freeze-drying and regeneration on the multiscale structure and rheological properties of the resulting hydrogels. We hypothesise that the removal of the arabinosyl substitutions will lead to increased interactions between xylan backbone chains and mechanically strengthen the subsequent hydrogels, similar to what can be achieved by freeze drying and regeneration in water. Wide and small angle X-ray scattering (WAXS and SAXS) techniques along with field emission scanning electron microscopy (FE-SEM) were used to investigate the hierarchical assembly and morphology of the hydrogels. Our results give greater insights into the mechanism of arabinoxylan hydrogel formation, showing that while the laccase-induced crosslinking is the driving force behind the gelation, other variables such as total solid content and chain interaction play a crucial role in the overall network assembly and derived rheological properties. We also show routes to manipulate hydrogel properties, using selective hydrolases to trim the arabinoxylan fibres, for tailored applications within prebiotic food products, using a green chemical approach.

2. Materials and methods

2.1. Materials

Wheat and rye bran were kindly provided by Lantmännen (Stockholm, Sweden). All chemical reagents and enzymes were purchased from Sigma-Aldrich (Hamburg, Germany), unless stated otherwise. Ferulic acid 5-5′ and 8-8' dehydrodimers were kindly donated by Prof. Florent Allais and Amandine Léa Flourat (AgroParisTech, Pomacle, France). α-L-Arabinofuranosidase from *Streptomyces thermoviolaceus* (SthAbf62A or GH62, EC 3.2.1.55 activity) was recombinantly produced by *Escherichia coli* BL21(λDE3) Codon Plus, and purified using Ni-NTA affinity chromatography followed by anion exchange chromatography on an Uno-Q column, as previously described (Wang et al., 2014). α-L-Arabinofuranosidase from *Bifidobacterium adolescentis* (GH43, EC 3.2.155 activity) was purchased from Megazyme (Bray, Ireland). Feruloylated arabinoxylan was extracted from wheat and rye bran using subcritical water extraction at 160 °C using tap water as extraction solvent, according to the method described by Ruthes et al. (Ruthes et al., 2020). After extraction, the arabinoxylans from wheat (WAX) and rye (RAX) were freeze-dried and powdered in a ball mill to facilitate

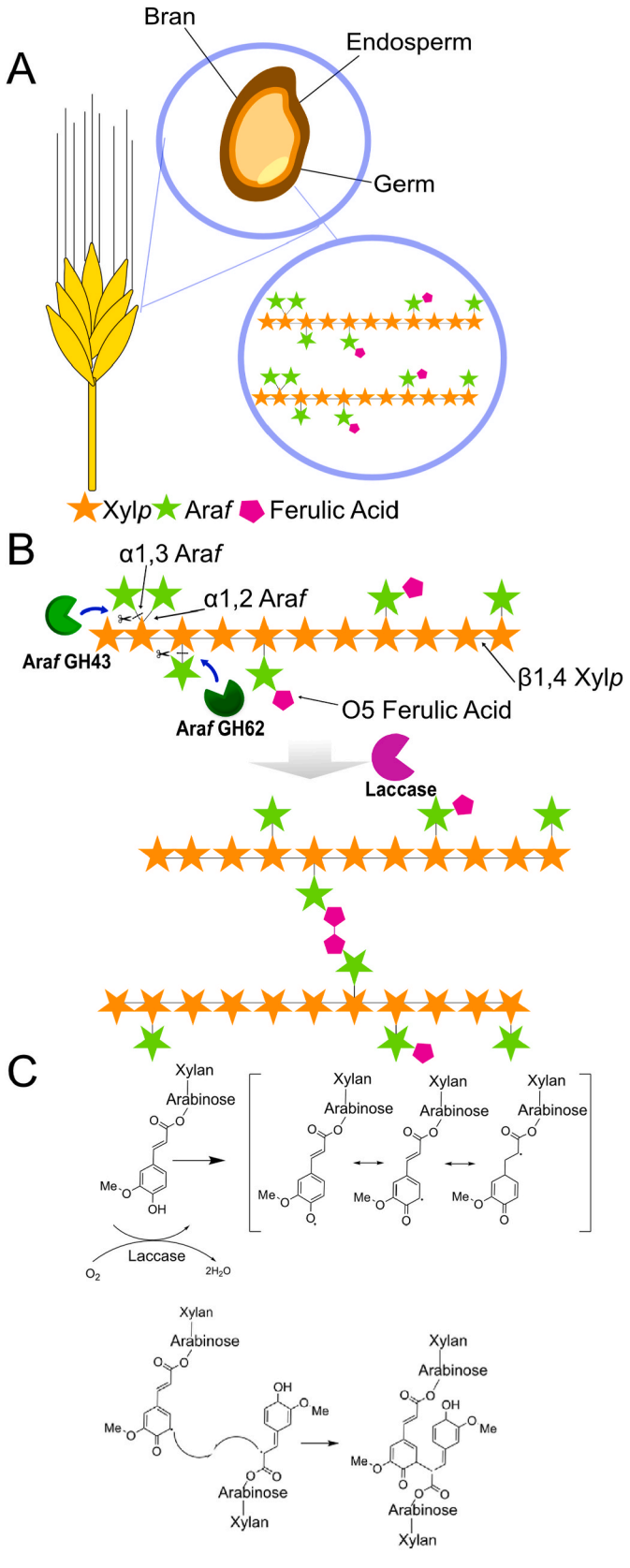

(caption on next column)

Fig. 1. A: Molecular structure of arabinoxylans in the bran of cereal grains. B: Molecular structure of arabinoxylan hydrogels treated with arabinofuranosidase and crosslinked by laccase. Arabinofuranosidases hydrolytically remove arabinosyl substitutions and laccase oxidises ferulic acid moieties. GH62 arabinofuranosidase remove O2- and O3-linked arabinoses from single-substituted xylans (Wang et al., 2014), whereas GH43 arabinofuranosidase hydrolyses O3-linked arabinose of double-substituted xylans (McKee et al., 2012). We hypothesise that treatment with GH62 and GH43 arabinofuranosidases will remove only terminal arabinose units, preserving the ones covalently bound to ferulic acid, which will act as sites for laccase oxidative crosslinking. C: Laccase-based crosslinking mode of action. As the laccase oxidises a hydroxyl group, a radical is formed that can occupy different positions through resonance stabilisation. Two radicals can couple and form a covalently linked ferulic acid dimer (Di-FA).

better solubility.

2.2. Hydrogel preparation and modification

2.2.1. Arabinose removal from arabinoxylan

For arabinose removal, GH43 and GH62 α-L-arabinofuranosidases were added to solubilised arabinoxylan (5 % w/v) at final concentrations of 0.01 mg/mL and 5.74 mg/mL respectively. Reactions were incubated simultaneously as the laccase-based crosslinking (see section 2.2.2 below) at 30 °C, 1500 rpm, overnight. Treated arabinoxylan was frozen at −80 °C overnight, and dried using a vacuum pump (Martin Christ, Osterode am Harz, Germany) to be stored for further use.

2.2.2. Laccase-based crosslinking and regeneration

Arabinoxylan crosslinking was performed using a laccase from *Trametes versicolor* (EC 1.10.3.2) (Sigma Aldrich). Arabinoxylans were first dissolved in MilliQ water (5 % w/v) by incubating at 95 °C and 1500 rpm for 45–60 min in a Thermomixer (Eppendorf, Denmark) and allowed to cool to room temperature. Laccase was added to a final concentration of 1675 nkat/mg arabinoxylan, incubated in a glass bottle (Ø20 mm) at 30 °C and 250 rpm overnight in a Thermomixer (Eppendorf, Denmark) until hydrogel formation has occurred. Hydrogels were frozen at −80 °C overnight, dried using a vacuum pump (Martin Christ, Osterode am Harz, Germany) and regenerated using 1 mL of MilliQ water (same volume as the crosslinking reaction) (Yilmaz-Turan et al., 2022).

2.3. Biochemical characterisation of the arabinoxylan extracts and hydrogels

2.3.1. Monosaccharide composition

Quantification of the monosaccharide composition was performed by trifluoroacetic acid (TFA) hydrolysis followed by high-performance anion exchange chromatography with pulsed amperometric detection (HPAEC-PAD). 1 mg of freeze-dried arabinoxylan was suspended in 1 mL of 2M TFA and heated to 120 °C for 3 h (De Ruiter et al., 1992; Ruthes et al., 2017). 100 μL of supernatant was air dried, resuspended in 1 mL of MilliQ water and filtered through Chromacol 17-SF-02(N) filters (Thermofisher, Waltham, MA, USA). The released monosaccharides (10 μL) were injected in the HPAEC-PAD system (Dionex ICS 6000, Sunnyvale, CA, USA), equipped with a CarboPac PA20 column maintained at 30 °C. The monosaccharides were separated at a flow rate of 0.4 mL/min using a gradient with MilliQ water (solvent A) and 200 mM NaOH (solvent B) and detected with post-column addition of 0.5 ml/min 200 mM NaOH. The column was equilibrated for 18 min with 1.2 % (v/v) solvent B, ramped up to 50 % (v/v) solvent B for 2 min and left for 10 min for sample elution. A standard curve was created using monosaccharides (fucose, arabinose, rhamnose, galactose, glucose, xylose and mannose), ranging from 0.005 g/L to 0.100 g/L.

2.3.2. Glycosidic linkage analysis

Glycosidic linkage analysis of the WAX and RAX extracts was performed as previously described (Ruthes et al., 2017). In brief, 1 mg of sample was dissolved in 400 μL of dimethyl sulfoxide (DMSO) with 20 mg of sodium hydroxide, to which 50 μL of methyl iodine (5 times) were added under continuous stirring. Samples were recovered in the organic phase after partition (3 times) of H_2O and dichloromethane and dried under N_2 in a sample concentrator (SBH200D/SBHCONC, Stuart). Dried samples were hydrolysed using 2 M TFA at 121 °C for 3 h, dried under N_2, reduced with $NaBD_4$ at 60 °C for 1h and acetylated with pyridine and acetic anhydride (1:1 v/v, 200 μL) at 100 °C for 30 min. The per-*O*--methylated alditol acetates (PMAAs) were extracted with ethyl acetate and quantified with GC-MS. The assignment of the PMAAs was performed comparing the retention times and the MS fragmentation patterns to known polysaccharide standards.

2.3.3. Quantification of phenolic acids and ferulic acid dehydrodimers

The phenolic acid content and dimers formed after arabinofuranosidase treatment and subsequent laccase-based crosslinking was measured after saponification of 10 mg of freeze-dried sample in 500 μL of 2M NaOH at 30 °C overnight, acidification by 100 μL 37 % HCL and partition with 2800 μL ethyl acetate (Menzel et al., 2019). The extracted phenolics were dried under nitrogen flow, suspended in methanol: 2 % acetic acid (1:1 v/v) and filtered through Chromacol 17-SF-02(N) filters (Thermofisher, Waltham, MA, USA). The filtered samples were analysed using an HPLC system (Waters 2695 separation module, Waters 2996 photodiode array detector; USA) coupled to a UV/Vis detector, equipped with a C18 guard column and an SB-C18 separation column (Zorbax SB-C18 5 μm particle size, 4.6 × 250 mm, Agilent, USA). The separation was performed using a gradient of 2 % acetic acid and methanol at 25 °C and 1 mL/min. A standard curve was created using *p*-coumaric acid, phenolic acid, caffeic acid, cinnamic acid, 5-5′ Di-FA and 8-8’ Di-FA, ranging from 0.005 g/L to 0.100 g/L.

2.3.4. Assessment of arabinose substitution pattern in WAX and RAX

To determine the pattern of arabinose substitutions on the xylose backbone, arabinoxylan structures were probed with xylanase enzymes of known specificity for differently substituted substrates. Arabinoxylan were dissolved in MilliQ water (5 % w/v) by incubating at 95 °C, under stirring for 45–60 min and allowed to cool to room temperature. GH10 xylanase BoXyn10A (E.C. 3.2.1.8) and GH8 xylanase *Cp*Xyn8A (E.C. 3.2.1.8) were individually added to a final concentration of 1 mg/g arabinoxylan and incubated at 50 °C under stirring overnight. The reaction was quenched at 95 °C for 10 min and the supernatant was collected and filtered through Chromacol 17-SF-02(N) filters (Thermofisher, Waltham, MA, USA). Samples were analysed using high-performance anion exchange chromatography with pulsed amperometric detection (HPAEC-PAD) system (Dionex ICS 6000, Sunnyvale, CA, USA), equipped with a CarboPac PA200 column. 10 μL of sample was injected into the column, with a temperature maintained at 30 °C and a flow rate of 0.4 mL/min. The gradient for the separation of different xylo-oligosaccharides used different solvents: MilliQ water (solvent A), 200 mM sodium hydroxide (solvent B) and 300 mM sodium acetate (solvent C). The samples were eluted with a 20 min gradient to 33 % (v/v) B + 66 % (v/v) solvent C. Linear xylo-oligosaccharides ranging from degree of polymerisation (DP) 1–6 units were used as qualitative standards at a concentration 0.1 mg/mL.

2.3.5. Molecular weight distributions

The molecular weight distributions of WAX and RAX were measured by size exclusion chromatography (SEC) coupled to a refractive index detector (Ruthes et al., 2017). Freeze-dried samples were dissolved in DMSO and LiBr solution (0.5 % w/w) at a concentration of 4 mg/mL and incubated at 60 °C overnight. The samples were filtered through Chromacol 17-SF-02(N) filters (Thermofisher, Waltham, MA, USA) and analysed by SEC (SECcurity 1260, Polymer Standard Services, Mainz, Germany) using in DMSO/LiBr (0.5 % w/w) with a flow rate of 0.5 ml/min at 60 °C using a GRAM PreColumn, 30 and 10000 analytical columns (Polymer Standard Services, Mainz, Germany). Calibration of the apparent molecular weight distributions was performed using pullulan standards between 342 Da and 1 300 000 Da (Polymer Standard Services, Mainz, Germany).

2.4. Functional and morphological characterisation of the hydrogels

2.4.1. Gel score and water absorption

The hydrogels were assessed visually and a qualitative score was implemented: a score of 0 indicated a liquid with an apparent viscosity as water; a score of 1 corresponded to a viscous-flowing liquid; a score of 2 showed the occurrence of solid aggregates suspended in liquid; a score of 3 corresponded with a free-standing loose hydrogel, and a score of 4 represented a firm free-standing hydrogel. The water absorption of hydrogels was gravimetrically determined after arabinofuranosidase and laccase treatment. Excess water was gently removed from the hydrogel surroundings and surface with fine tissues and the reduction in weight was used to determine the level of water retention. The total solid content of the hydrogels was calculated gravimetrically based on the water absorption data.

2.4.2. Rheological measurements

Rheological measurements on arabinoxylan hydrogels were performed on a strain-controlled rheometer (Discovery HR 20, TA Instruments, New Castle, DE, USA) at 25 °C, using a 20 mm sandblasted parallel plate geometry. The viscoelastic properties were analysed using small amplitude oscillatory shear test with a frequency sweep ranging between 0.6 and 125 rad/s, a 0.5 % oscillation strain and a constant axial force of 0.15 N (Yilmaz-Turan et al., 2022).

2.4.3. Wide-angle (WAXS) and small angle X-ray scattering (SAXS)

WAXS and SAXS measurements were performed on WAX and RAX hydrogels with and without arabinofuranosidase treatment, before and after freeze drying and regeneration. WAXS measurements were conducted on a SAXSLAB Mat:Nordic (Denmark) benchtop instrument with a Cu Kα radiation source (λ = 1.54 Å) and a Pilatus 300K detector (Dectris, USA). The sample-to-detector distance was 130 mm, covering a q-range of 0.07 $Å^{-1}$ to 2.20 $Å^{-1}$. q-calibration was performed using LaB6 powder. Hydrogel samples were mounted onto a sandwich cell holder with an O-ring of thickness 1.78 mm (also sample thickness), sealed on both sides with Kapton windows each of thickness 0.02 mm. Each sample was measured in vacuum with an exposure time of 1800 s. The signal of water held in the same sandwich cell holder setup was used for background subtraction.

Similarly, SAXS measurements of the arabinofuranosidase treated RAX and WAX dispersions were performed on the same equipment as the WAXS measurements with sample-to-detector distances of 480 mm and 1530 mm, covering a q-range of $0.0036 \leq q \leq 0.78$ $Å^{-1}$, and using the same setup for sample mounting. The SAXS measurements on the hydrogels were performed using a SAXSPoint 2.9 instrument (Anton Paar GmbH, Graz, Austria) with a Cu Kα radiation source (λ = 1.54 Å) and an Eiger R 1m Horizontal detector (Rigaku Corporation, Tokyo, Japan). The sample to detector distance was 561.9 mm, with an acquisition time of 30 min and a constant temperature of 25 °C. The scale of the data was received at a q-range of $0.007 \leq q \leq 0.52$ $Å^{-1}$. All samples were placed in a multi-paste holder, sealed with an O-ring and mica windows. Data reduction was performed using the SAXSGUI software (version 2.27.03). The windows or empty capillary, and the water backgrounds were subtracted in the WAXS and SAXS data using a Python script (Jupyter Notebook 7.0.8).

2.4.4. Field emission scanning electron microscopy (FE-SEM)

Freeze dried hydrogels were prepared for microscopy through cryo-cracking (Lundin et al., 1998) where they were frozen in liquid nitrogen

and carefully broken apart using a metal spatula. Samples were dried overnight in a vacuum pump as described above. The structure of the samples was analysed using a field emission scanning electron microscope (FE-SEM; Hitachi S-4800, Tokyo, Japan). Samples were placed on conductive carbon tape and analysed at a voltage of 1 kV and a current of 10 μA (Birdsong et al., 2024).

3. Results and discussion

3.1. Biochemical characterisation of the starting WAX and RAX substrates

Arabinoxylans from wheat (WAX) and rye (RAX) were extracted from their respective bran sources using subcritical water extraction. Their monosaccharide composition was analysed using HPAEC-PAD after acid hydrolysis (Supplementary Fig. S1A, Supplementary Table S1). Both WAX and RAX extracts showed high AX purity of around 730–750 mg/g (Table 1). The extracts also contained a significant fraction of glucose, likely from mixed-linkage β-glucan (MLG) and residual endosperm starch (Arens, 2015; Rudjito et al., 2020; Stevenson et al., 2012). The arabinoxylans in the WAX and RAX extracts share a similar degree of substitution, with low ratios of arabinose to xylose (A/X ratio) of around 0.2 (Table 1). Such A/X ratios are lower than those previously reported for AX extracted in alkaline conditions, due to the hydrolytic nature of subcritical water that may cause degradation of the labile arabinofuranose moieties, but preserving the ferulic acid moieties (Ruthes et al., 2017). To complement the monosaccharide analysis, glycosidic linkage analysis was performed (Supplementary Fig. S1B and Supplementary Table S2). WAX and RAX extracts show slight differences in the relative amount of single and double substitutions. Specifically, RAX showed a higher relative abundance of single-substituted Xyl*p* (3,4-Xyl*p*) units compared to WAX, whereas WAX showed slightly higher relative abundance of double-substituted Xyl*p* (2,3,4-Xyl*p*) units (Table 1). To investigate the distribution of arabinose substitutions on the xylan backbone, WAX and RAX were incubated with a GH10 xylanase (BoXyn10A), and the oligosaccharide profile was qualitatively assessed using HPAEC-PAD (Supplementary Fig. S1C). The oligosaccharide profiles of WAX and RAX extracts were comparable, suggesting similar arabinose substitution pattern on the arabinoxylans.

Table 1
Biochemical characterisation of WAX and RAX extracts. NOTE: Standard deviation between brackets ().

	WAX	RAX
Total carbohydrate (mg/g) [a]	836.6 (61.4)	967.1 (81.9)
Arabinoxylan (mg/g)[a]	732.2 (52.4)	750.8 (67.8)
A/X ratio[a]	0.31 (0.00)	0.37 (0.01)
4-Xyl*p*[b]	80	79
2,4-Xyl*p*[b]	4	3
3,4-Xyl*p*[b]	10	14
2,3,4-Xyl*p*[b]	6	4
Starch (mg/g)[c]	26.6 (2.7)	48.9 (2.9)
β-glucan (mg/g)[d]	65.9 (7.3)	158.8 (12.3)
Ferulic acid (mg/g)[e]	15.3 (0.7)	11.3 (0.1)
X/FA molar ratio[f]	50.0	70.7
M_p (kDa)[g]	88.4	110.6

[a] Calculated from the monosaccharide analysis (Supplementary Table S1).
[b] Substitution pattern of xylose units in AX backbone calculated from the glycosidic linkage analysis (Supplementary Table S2), normalised to 100 Xylp backbone units.
[c] Starch content calculated enzymatically using the Total Starch Kit.
[d] β-glucan calculated subtracting the starch content from the total Glc content from the monosaccharide analysis (Supplementary Table S1).
[e] Ferulic acid content in arabinoxylan extract calculated after HPLC-UV (Supplementary Table S3).
[f] Molar ratio of xylose units and ferulic acid, calculated from the composition.
[g] Molecular weight of arabinoxylan calculated from the peak maximum of the distribution using SEC-DRI (Supplementary Fig. S1E).

The phenolic contents of WAX and RAX were determined by HPLC-UV after saponification (Supplementary Fig. S1D, Table S3). WAX showed a higher amount of ferulic acid compared to RAX, with values of 15.3 and 11.3 mg/g, respectively (Table 1). This indicated that WAX has on average one ferulic acid moiety every 50 Xyl*p* units, whereas RAX had one ferulic acid every 70 Xyl*p* units. Both extracts contained a similar abundance of Di-FA structures, in the form of 8-8′ and 5-5′ dimers. It must be stated that the only dimers that could be quantified were 8-8′ and 5-5’ due to availability of synthesised standards. Lastly, the molar mass distributions to of WAX and RAX were analysed by size exclusion chromatography (Supplementary Fig. S1E). Subcritical water preserved the polymeric structure of WAX and RAX, with RAX showing slightly higher molar mass than WAX (Table 1).

In short, the major differences between RAX and WAX substrates seem to be the larger amount of MLG in the RAX extract, and the higher ferulic acid content in the WAX extract, whereas the xylan substitution pattern are fairly similar and only show slight differences in the extent of single- and double-substituted units along the xylan backbone. Previous studies suggest that the patterns of substitution occur in clusters and are not randomly distributed along the arabinoxylan backbone, with highly substituted and less substituted regions interspaced (Rudjito et al., 2023; Viëtor et al., 1994). This suggests that slight local differences in the substitution pattern might have potentially larger effects on the properties of the arabinoxylan chains.

3.2. Impact of arabinofuranosidase treatment on arabinoxylan structure

It has previously been shown that regeneration of freeze-dried arabinoxylan hydrogels leads to mechanically stronger hydrogels, which was attributed to enhanced interactions along the arabinoxylan polymers that contribute to supramolecular network formation (Yilmaz-Turan et al., 2022; Zhang et al., 2019). Our hypothesis is that enzymatic removal of terminal arabinosyl residues from xylans, without removing the ferulic acid moieties, will lead to a more exposed xylan backbone, favouring supramolecular interactions and hence stronger hydrogels upon regeneration. We first studied the extent to which WAX and RAX could be debranched by different arabinofuranosidase treatments. Kinetic assays were performed with WAX and RAX using arabinofuranosidases from the glycosyl hydrolase families GH62 and GH43 (Supplementary Figs. S2 and S3), which remove singly-substituted and doubly-substituted arabinoses from the xylan backbone, respectively (McKee et al., 2012; Wang et al., 2014). The same kinetic assay was initially performed with a GH51 α-arabinofuranosidase from Aspergillus niger (Megazyme, Ireland), previously shown to remove single-substituted arabinose from AX oligosaccharides (McGregor et al., 2020), and no arabinose release was detected (data not shown), indicating that GH51 could not remove arabinose from polymeric WAX and RAX. Hence we decided to move ahead with the GH62 and GH43 enzymes instead. We initially screened several enzyme concentrations for GH62 and GH43 to release arabinose from WAX in diluted substrate concentrations (Fig. S2) and these optimal enzyme concentrations were tested for both WAX and RAX at the final substrate concentration (Fig. S3). The GH62 reached reaction completion after 6 h at an enzyme concentration of 5,74 mg/mL, whereas GH43 reached reaction completion after 24 h with an enzyme concentration of 0,01 mg/mL (Figs. S2 and S3). Subsequent enzyme dosing showed no increase of released arabinose (data not shown), indicating that no more arabinose was accessible for cleavage. For both WAX and RAX extracts, more arabinose is released with GH62 compared to GH43 (Fig. 2A, Table S4), which is as expected considering the larger amount of single-substituted xylose compared to double-substituted (Table 1). Co-incubating the enzymes releases more arabinose compared to if they were incubated separately, showing clear synergistic effect (Fig. 2A–Table S4) as the removal of one arabinose moiety by GH43 allows the remaining one to be cleaved by GH62 (Sørensen et al., 2006). We also assessed the phenolic content in solution after the arabinofuranosidase treatment of

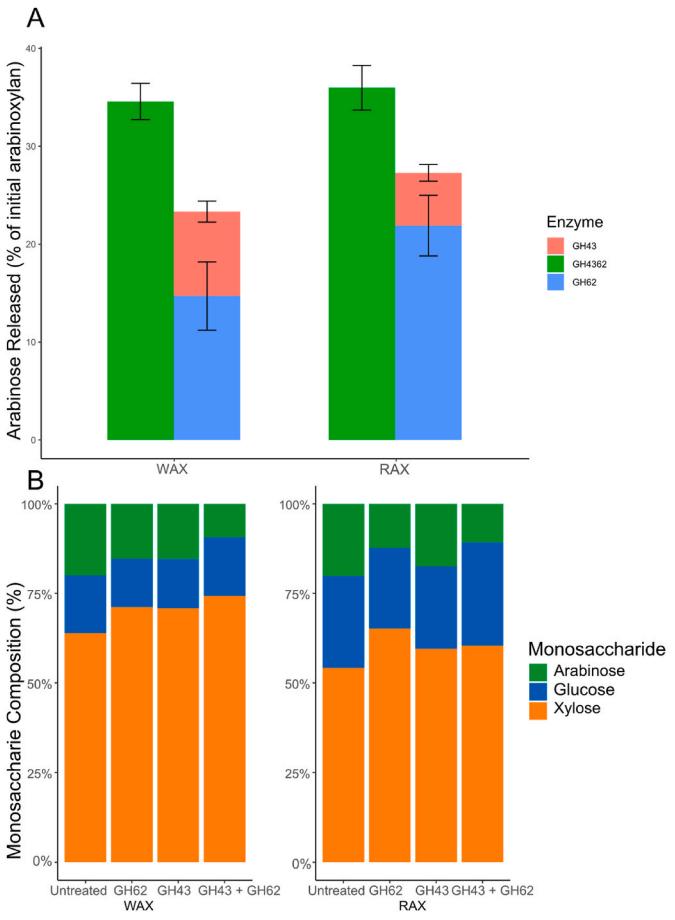

Fig. 2. Arabinofuranosidase treatment effect on WAX and RAX extracts. A: Arabinose released after arabinofuranosidase treatment. Treating arabinoxylan with both enzymes synergistically release more arabinose than treated separately. B: Monosaccharide composition of WAX and RAX extracts after arabinofuranosidase treatment. Arabinose content in the AX substrates is reduced after each enzymatic treatment.

WAX and RAX extracts and no ferulic acid or dimers (di-FAs) were detected (data not shown). This confirms that neither arabinofuranosidase can remove arabinose subunits with a phenolic acid linked to them, as the ferulic acid hinders access to the narrow pocket of the active site of the arabinofuranosidases (Wang et al., 2014). In turn, this indicates that the number of potential crosslinking sites in WAX and RAX is not altered by arabinofuranosidase treatment.

The arabinose content in the WAX and RAX after arabinofuranosidase treatment was measured (Fig. 2B and Supplementary Table S4), and indicated that a distinct portion of arabinose remains in both WAX and RAX. Some of these arabinose moieties are expected to remain, as they are linked to ferulic acid and thus inaccessible for the arabinofuranosidases. However, the combined GH62 and GH43 treatments were not able to remove all the terminal arabinoses from the WAX and RAX. We estimated the amount of remaining non-feruloylated arabinose units in the arabinoxylans by subtracting the total arabinose units (in mol%) after arabinofuranosidase treatment (calculated from the monosaccharide analysis, Supplementary Table S4) with the total arabinose units carrying a ferulic acid moiety (estimated from the ferulic acid content in mol%, Supplementary Table S3); the WAX and RAX extracts respectively showed 7 and 11 non-feruloylated arabinose units per 100 xylose units. We hypothesise that the progressive removal of arabinose units leads to aggregation of the AX chains, further hindering the accessibility of the arabinofuranosidases. Indeed, a lower arabinose content has been reported to increase the flexibility of the xylan chains in AX and worsen water interaction (Janewithayapun et al., 2025), which could explain the increased AX agglomeration and reduced enzyme accessibility. The difference in non-feruloylated arabinose units could potentially play a role in the conformation of the arabinoxylan chains, thus affecting the efficacy on the arabinofuranosidases.

3.3. Phenolic content of arabinoxylan after laccase and arabinofuranosidase treatment

When preparing hydrogels, before the addition of the laccase, the WAX and RAX extracts were heated in MilliQ water at 95 °C for 60 min to facilitate their dissolution. It was noted that if the arabinoxylans were dissolved at room temperature, a hydrogel would not form following laccase addition (data not shown). One explanation could be that heating would disrupt supramolecular interactions between arabinoxylan chains, thus making more ferulic acid accessible to laccase-mediated oxidation and crosslinking, and contribute to hydrogel formation (Bakó et al., 2017; Zheng et al., 2024). Indeed, some xylans, while appearing dissolved to the naked eye, can form aggregates in solution (Kishani et al., 2019).

To determine the impact of arabinose removal on laccase-based crosslinking of WAX and RAX extracts, phenolic content was measured in the untreated extracts, arabinoxylan hydrogels with laccase (as control) and arabinoxylan hydrogels pretreated with arabinofuranosidases prior to laccase crosslinking (Fig. 3, Supplementary Table S3). The Di-FAs 8-8′ and 5-5′ were quantified using synthetic standards. While other dimers could not be confirmed due to lack of standards, the HPLC chromatograms showed distinct peaks arising after laccase treatment that do not correspond to either 8-8′ or 5-5 dimers, suggesting the occurrence of other putative dimer structures of ferulic acid. The abundance of putative dimers can be roughly estimated by subtracting the amount of 8-8′ and 5-5′ dimers from the total amount of decreased ferulic acid content (data not shown). Because of the difficulty to measure all products from the laccase reaction (including oxidised ferulic acid not undergoing dimerization, and larger crosslinked trimer- and tetramer-FA), using the decrease in ferulic acid content is used as an approximation of the crosslinking activity of the different samples. As expected, the amount of ferulic acid decreases for both WAX and RAX after laccase treatment, along with an increase of both 8-8′ and 5-5’ dimers and the other putative dimer-, trimer- and tetramer-FAs and (Fig. 3). Interestingly, the decrease in ferulic acid content in samples treated only with the laccase was more significant for the RAX compared to the WAX, despite the higher ferulic acid content in WAX. Moreover, WAX and RAX show different phenolic profiles depending on which combination of arabinofuranosidases they were treated with. WAX treated with GH43 alone showed a substantial decrease in ferulic acid content after laccase-mediated oxidation, whereas the effect was smaller on RAX treated with GH43. Conversely, WAX treatment with both GH43 and GH62 hinder ferulic acid oxidation by laccase to a larger extent. Interestingly, treatment of WAX with GH62 alone did not seem to largely influence the extent of ferulic acid oxidation, whereas for RAX, it greatly reduced the amount of crosslinking compared to the control laccase treatment.

These differences in ferulic acid content following laccase oxidation in substrates exposed to arabinofuranosidase treatment can be attributed to different levels of accessibility of the laccase to the ferulic acid in both WAX and RAX substrates. Although ferulic acid reactivity is not mechanistically linked to structural factors of the AX chain (e.g., arabinose substitution patterns, chain aggregation), the accessibility of the laccase enzyme to its substrate (ie ferulic acid) is. One explanation is the potential steric hindering effect of adjacent arabinoses on the accessibility of laccase to bound ferulic acid moieties. It is established that the conformation of side chains may affect protein interactions with polysaccharides (Watkins et al., 2016), and polysaccharide substitution may inhibit the binding of laccase (Liu et al., 2021). Indeed, WAX has slightly higher double-substituted Ara*f* units compared to RAX, and the use of a

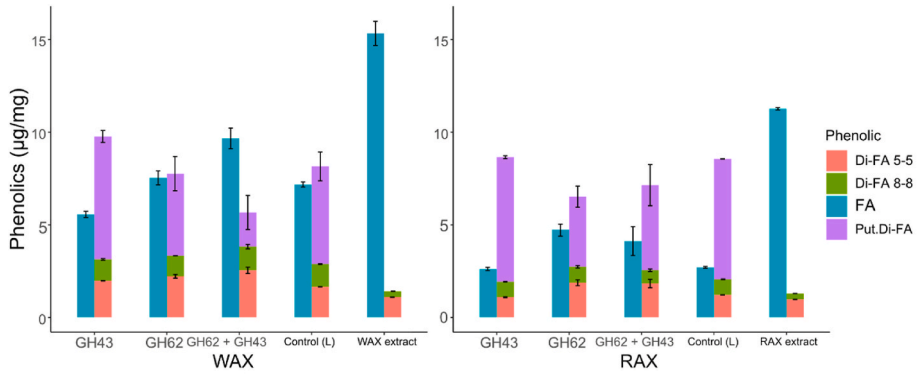

Fig. 3. Phenolic composition of WAX and RAX extracts, the hydrogels after laccase crosslinking (Control (L)) and the laccase-crosslinked hydrogels after arabinofuranosidase treatments. Laccase treatment decreased the amount of ferulic acid due to its oxidation and increases the amount of dimers (Di-FAs). Arabinofuranosidase treatment lowers the extent of ferulic acid oxidation by the laccase.

GH43 arabinofuranosidase in WAX seems to increase the extent of ferulic acid oxidation by laccase. Another explanation could be related to the presence of longer unsubstituted stretches in WAX compared to RAX, which could induce chain aggregation limiting the available ferulic acid for the laccase. Indeed, the fact that less ferulic acid is oxidised in both WAX and RAX when they have been previously treated with both GH62 and GH43 could be due to occlusive backbone interactions in the de-arabinosylated xylan (Yu et al., 2019), causing aggregation in solution (Kishani et al., 2019). In conclusion, the results suggest that both the substitution pattern and the conformation (aggregation) of the arabinoxylan chains influence laccase accessibility and the occurrence of covalent crosslinks, which in turn will affect the functional properties of the hydrogels.

3.4. Previous arabinofuranosidase treatment tunes the rheological properties of laccase-crosslinked hydrogels upon regeneration

The gelling properties of the laccase-crosslinked arabinoxylans with and without arabinofuranosidase treatment before and after regeneration were initially evaluated qualitatively using a “gel score” (Fig. 4A). Arabinofuranosidase treatments greatly affected hydrogel formation for WAX prior to regeneration. Without any arabinofuranosidase treatment, WAX formed a loose hydrogel upon addition of laccase, whereas pre-treatment with GH62 or GH62+GH43 arabinofuranosidases resulted in a viscous liquid behaviour, suggesting worse gelation after arabinose removal. RAX hydrogels were less affected by the arabinofuranosidase treatment. RAX samples pre-treated with GH62 before laccase reaction resulted in a partially loose hydrogel, whereas all other treatments resulted in firm solid hydrogels similar to those obtained from untreated RAX. These observations support the results from the phenolic acid composition (Fig. 3). As previously observed (Yilmaz-Turan et al., 2022), freeze-drying and regeneration improved the gelling properties for all samples, resulting in firm free-standing hydrogels, except for WAX hydrogels treated with GH43+GH62 that showed softer consistency.

To assess the water absorption capacity of the hydrogels, WAX and RAX hydrogels were weighed before and after freeze drying and regeneration, with and without the arabinofuranosidase treatment (Fig. 4B). Prior to freeze drying, arabinofuranosidase treatment moderately change the water absorption capacities of the WAX and RAX hydrogels. After freeze drying and regeneration, however, a clear trend can be seen in both WAX and RAX hydrogels, with a reduced water absorption when more arabinose is removed by arabinofuranosidases. This indicates that arabinose removal in conjunction with freeze drying and regeneration drastically reduces the swelling capacity of the hydrogels and their water holding capacity and thus considerably altering their total solid content up to 4-fold for the case of RAX (Table 2).

The viscoelastic properties of the hydrogels were further studied, and the storage modulus, G′, and loss modulus, G″ of the hydrogels are shown in Fig. 4C. The measured samples exhibited in general larger values of G′ over G″, indicating that all of them can be defined as hydrogels within the frequency range tested. Only the laccase-crosslinked WAX sample treated with GH62 and GH43 before regeneration showed very low values and potentially in the limit of the detection of the rheometer, in agreement with the reported hydrogel score. Regeneration resulted in a higher G’ modulus for all WAX and RAX samples compared to the non-regenerated samples, which can be attributed to a network clustering effect of the polysaccharide chains caused by the freeze-drying process and the increase in total solid content, as previously described (Vansteenkiste et al., 2004; Yilmaz-Turan et al., 2022). In order to evaluate the contribution of the increase in total solid content caused by the regeneration process, we have compared the rheological properties of a laccase-crosslinked WAX hydrogel at 7.5 wt% before regeneration matching the same total solid content reached after regeneration (Table 2). The physical reorganisation of the polysaccharide chains induced by the freeze-drying and regeneration process indeed increases both the storage and loss moduli compared with the non-regenerated hydrogel at the same total solid content (Supplementary Material Fig. S4), indicating that the increase of solid content is not the solely factor contributing to the viscoelastic processes.

Interestingly, enzymatic removal of arabinose had diverging effects on the rheological properties of WAX and RAX hydrogels. RAX hydrogels showed the highest G′ and G″ moduli when treated with both GH43 and GH62 compared with the samples without any arabinofuranosidase treatment. This result confirms the original hypothesis of this study, as arabinose removal from RAX seem to promote intermolecular interactions between AX chains in the hydrogel network and lower water retention, resulting in a higher G’. Treatment with only a GH43 arabinofuranosidase did not alter the rheological properties of the RAX hydrogels compared to the laccase control, in agreement with the lower amount of double-substituted Ara*f* units in RAX compared to WAX. Contrarily, WAX hydrogels without any arabinofuranosidase treatment showed the highest value of G′, especially for the regenerated samples, with the lowest values of G′ and G″ for the WAX samples treated with both GH43+GH62 enzymes. This agrees with the observations from the phenolic acid analysis, as the removal of arabinose has an impact on the extent of laccase oxidation caused by potential aggregation. RAX extract contains higher MLG content than WAX, and different MLG contents may contribute to the rheological properties of arabinoxylan hydrogels due to physical interactions between the polysaccharide chains (Brummer et al., 2014).

In order to further investigate the factors influencing the viscoelastic properties of the hydrogels, the G′ and G″ for all samples at a angular

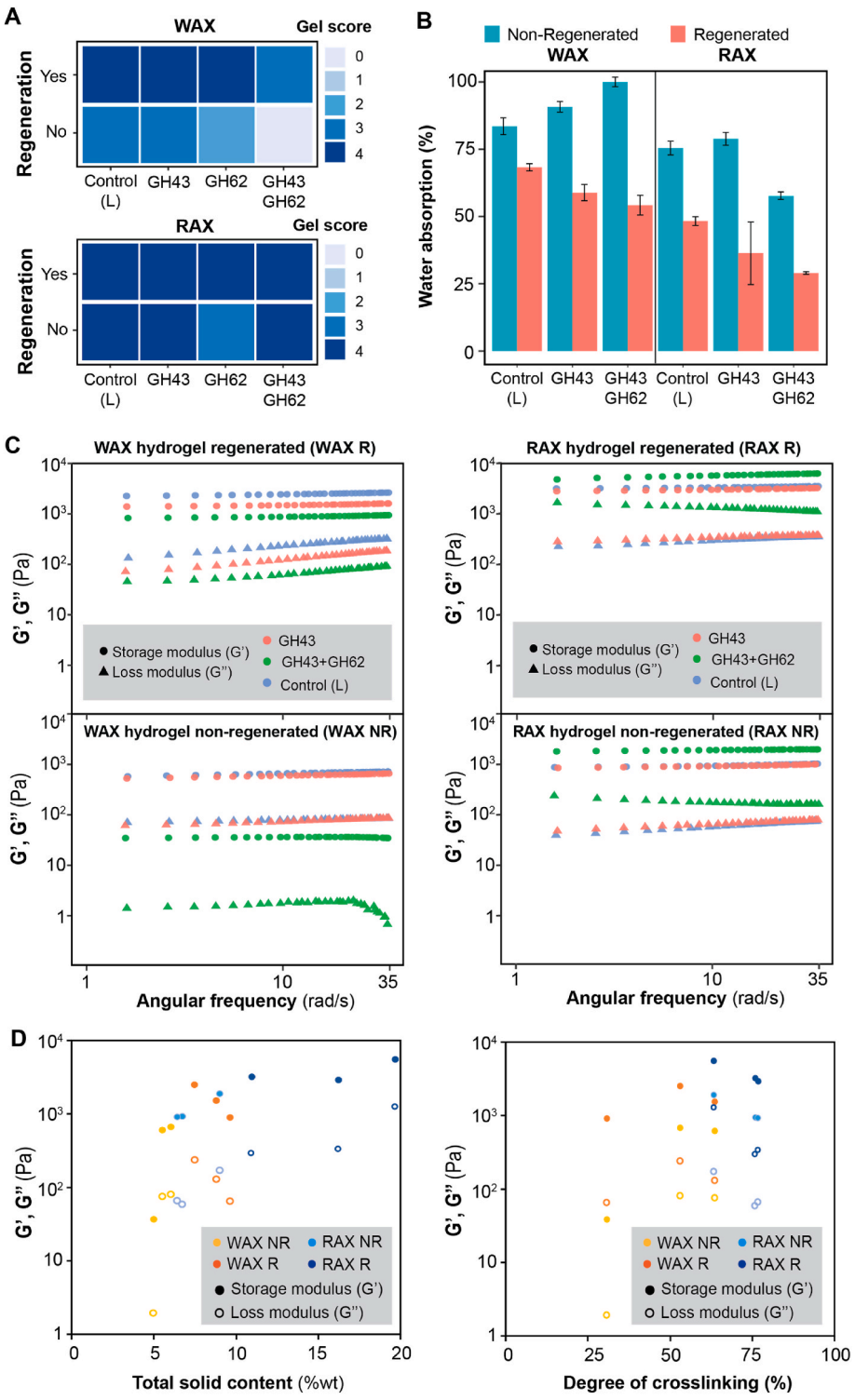

Fig. 4. A) Qualitative gel score (between 0 and 4). A score of 0 indicated a completely liquid with an apparent viscosity like water; a score of 1 corresponded to a viscous flowing liquid; a score of 2 showed the occurrence of solid pieces suspended in liquid; a score of 3 corresponded with a free-standing loose hydrogel, and a score of 4 represented a firm free-standing hydrogel. B) Water absorption of WAX and RAX hydrogels. C: Viscoelastic properties of WAX and RAX hydrogels: storage modulus (G′) and loss modulus (G″). Data shown between 1 and 35 rad/s as the oscillation torque and displacement were in phase at those frequencies. D) Correlation between the storage and loss moduli (at an angular frequency of 10.6 rad/s) with the total solid content and the degree of crosslinking (Table 2).

frequency of 10.6 rad/s were correlated with the total solid content and the degree of crosslinking (Table 2). In general, G'and G''correlate well with the total solid content, especially for the RAX hydrogels, indicating that the hydration effects caused by the arabinose removal and the freeze drying/regeneration seem to control the rheological properties of the hydrogels once they are formed. On the other hand, the degree of crosslinking seemed to be the determining factor for the rheological properties of the WAX hydrogels. Based on these results, we propose that while laccase-based crosslinking is the main force behind the gelation process, other factors such as hydration (influencing the solid content)

Table 2
Physico-chemical and structural properties of the laccase-crosslinked WAX and RAX hydrogels.

Sample	Degree of crosslinking (%)[a]	Solid content (wt %) [b]	G' (Pa) [c]	G'' (Pa)[c]	Porod Exponent
WAX L	53.2	6.0 ± 0,2	665	79	3.58 ± 0.02
WAX LR	53.2	7.5 ± 0.2	2462	238	3.46 ± 0.02
WAX GH43 L	63.7	5.5 ± 0.1	600	74	n.d.
WAX GH43 LR	63.7	8.8 ± 0.5	1496	127	n.d.
WAX GH43GH62 L	30.9	5.0 ± 0.1	36	2	3.57 ± 0.03
WAX GH43GH62 LR	30.9	9.6 ± 0.7	882	64	3.63 ± 0.01
RAX L	76.0	6.7 ± 0.2	920	58	3,32 ± 0,02
RAX LR	76.0	10.9 ± 0.4	3229	293	3.40 ± 0.01
RAX GH43 L	76.8	6.4 ± 0.2	903	65	n.d.
RAX GH43 LR	76.8	16.2 ± 0.2	2912	334	n.d.
RAX GH43GH62 L	63.4	9.0 ± 0.2	1879	171	3.31 ± 0.02
RAX GH43GH62 LR	63.4	19.7 ± 0.4	5567	1284	3.39 ± 0.01

NOTE: n.d. (not determined); L (laccase crosslinked hydrogels), R (freeze-dried and regenerated hydrogels).
[a] Calculated based on the decrease of the ferulic acid content after laccase-based crosslinking (Fig. 3).
[b] Calculated based on the water absorption data after freeze drying(Fig. 4B).
[c] Values of the storage and loss moduli at an angular frequency of 10.6 rad/s (Fig. 4C).

and the occurrence of physical interactions between arabinoxylan chains (influencing the network organisation) influence the overall rheological properties of the hydrogels before and after regeneration. These processes seem to occur simultaneously during hydrogel formation and contribute in a conflicting way to the behaviour and structure of the hydrogels.

3.5. *Arabinose removal affects the hierarchical assembly of laccase-crosslinked hydrogels*

To further investigate the diverging rheological properties of the WAX and RAX dispersion and hydrogels upon arabinofuranosidase treatment, their multiscale network assembly was investigated by complementary WAXS and SAXS analysis. The WAXS diffractograms for all arabinoxylan samples exhibit sharp peaks (Fig. 5A, Table S5) which indicate the occurrence of ordered regions, in agreement with the results provided for xylan hydrate by Nieduszynski and Marchessault (1972) and (Johnson et al., 2023). Interestingly, we observe differences between WAX and RAX dispersions: the RAX dispersions have lower intensity and broader peaks suggesting that WAX have an overall higher degree of order than RAX. In the WAX dispersions, we observe no conclusive change between the arabinofuranosidase treated and untreated samples in this atomic length-scale. Although there are differences in the intensity, the differences are not clear enough to rule out other factors such as variations in the dispersion concentration between capillaries. In the case of the RAX dispersion, we observe a difference in both peak shape and intensity, especially between 1 $Å^{-1}$ and 1.5 $Å^{-1}$. This suggests that even after taking into account concentration variations, the WAXS data still suggests that the enzyme treated sample tends to phase separate/sediment more, and that the arabinofuranosidase treated RAX sample is less hydrated, in agreement with the lower water absorption shown in Fig. 4B. The differences between the RAX dispersions also suggest that arabinofuranosidases can access RAX more easily owing to the lower degree of order in the starting substrate.

When comparing the hydrogels, WAX hydrogels have as well a higher degree of ordering than RAX hydrogels, as observed in the dispersions. The sample form and sample holder geometry provides better control over concentration variations compared to dispersions in capillaries. Therefore, an increase in ordering of both RAX and WAX hydrogels upon freeze drying and regeneration of the arabinofuranosidase-treated hydrogels can be observed, by increased peak intensities and lower amorphous background. This increase in order suggests that the combination of regeneration and arabinofuranosidase treatment leads to larger backbone interactions, as previously proposed (Yilmaz-Turan et al., 2022). This increase in order is also partially observed in the arabinofuranosidase-treated RAX hydrogels, even without regeneration, adding further evidence that these enzymes have better access in RAX, as observed in the dispersions.

In parallel, we performed SAXS experiments on the WAX and RAX dispersions and hydrogels to investigate the influence of arabinofuranosidase treatment on their nanoscale organization (Fig. 5B, Supplementray Material Fig. S5). The SAXS patterns of the dispersions and the hydrogels are very similar in the lower q region (<0.03 $Å^{-1}$), except for the arabinofuranosidase WAX dispersion, which seems to have an upturn at the lowest q-values (q < 0.01 $Å^{-1}$). However, studies at a lower q range would be needed to assess the nature of this upturn suggesting larger aggregation. In the region between 0.03 and 0.07 $Å^{-1}$, the values of the Porod exponents for all samples are between 3 and 4 (Table 2), suggesting a compact 3D structure in all cases. For the untreated RAX dispersion and hydrogels, the Porod exponent was lower compared to WAX samples, and to enzyme treated samples. This lower Porod exponent, indicating less compact dispersions, supports the larger effect of enzymatic treatment on the RAX samples. Lastly, between 0.7 and 1.5 $Å^{-1}$ we observe a small broad peak in the arabinofuranosidase-treated RAX dispersion and hydrogels that is not observed neither in the WAX, nor in the untreated RAX. This peak, similar to that observed in low-substituted AX from wheat bran prepared via chemical fractionation (Janewithayapun et al., 2025), indicates that arabinofuranosidase treatment has an impact on the structure of RAX. In summary, these results suggest that gelation with laccase does not alter the nano structure of the arabinoxylans, whereas arabinofuranosidase treatment affects the structure of RAX at the nano scale.

The overall investigation of the multiscale assembly of the hydrogels by combined WAXS and SAXS measurements provide some correlation with the viscoelastic properties of the different hydrogels. The combination of arabinose removal, freeze-drying and regeneration yielded the highest degree of ordering in both WAX and RAX hydrogels but highest viscoelasticity only in RAX hydrogels, showing that while the degree of ordering of arabinoxylan hydrogels have a strong correlation with their viscoelastic properties, it is not the sole variable responsible. In parallel, the results by SAXS indicate that the network organisation at the q range of the experiments is not largely affected by arabinofuranosidase treatment and regeneration.

The morphological changes of the freeze-dried WAX and RAX hydrogels upon arabinofuranosidase treatment were analysed using field emission scanning electron microscopy (FE-SEM). The reference laccase-crosslinked WAX hydrogels exhibit an interconnected polymeric network and a highly porous microstructure with the occurrence of both larger and smaller pores (Fig. 6A). Arabinofuranosidase treatment before laccase-based crosslinking of the WAX hydrogels lead to a less compact structure and loss of network integrity (Fig. 6B). In parallel, laccase-crosslinked RAX hydrogels showed a more compact and structured network after the arabinofuranosidase treatment (Fig. 6C). Interestingly, arabinofuranosidase treatment caused a drastic decrease in the pore size of the RAX hydrogels and a smoother surface pore pattern compared to the RAX controls (Fig. 6D). The FE-SEM images reveal that the arabinofuranosidase treatment seem to disrupt the hierarchical

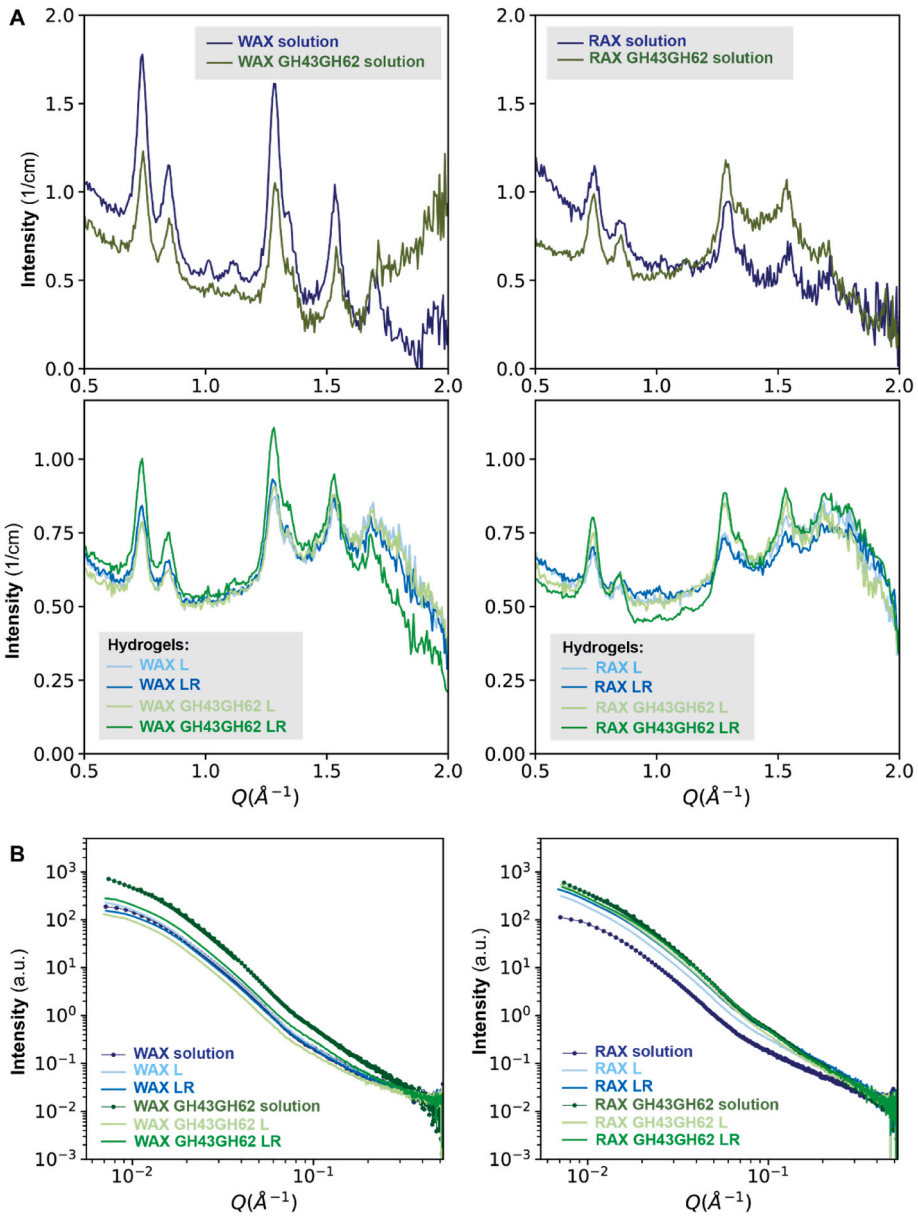

Fig. 5. X-ray scattering profiles of WAX and RAX solutions and hydrogels. A. Wide-angle X-ray scattering (WAXS). B. Small-angle X-ray scattering (SAXS). Sample nomenclature corresponds with the samples in Table 2.

organisation of the WAX hydrogels, whereas the RAX hydrogels achieve a more tightly packed and compact network structure. This coincides with the rheological measurements described above, with WAX hydrogels having lower viscoelasticity with arabinose removal and RAX hydrogels showing the opposite behaviour. This reinforces our results, indicating that the arabinofuranosidase treatment of arabinoxylan hydrogels affects their hierarchical assembly and microstructure, which in turn impact their overall rheological properties.

4. Conclusion

In this work we demonstrate that the rheological properties of hydrogels produced through laccase-based crosslinking of feruloylated arabinoxylan derived from wheat (WAX) and rye (RAX) brans can be fine-tuned using arabinofuranosidases and subsequent freeze-drying and regeneration. The synergistic activity of arabinofuranosidases from families GH43 and GH62 results in the successful removal of arabinose from WAX and RAX without affecting the ferulic acid moieties. Interestingly, the removal of arabinose from WAX and RAX influence differently the structure and rheological properties of their respective laccase-crosslinked hydrogels. Arabinose removal from RAX hydrogels prior to laccase-based crosslinking resulted in hydrogels with higher storage and loss moduli, before and after regeneration, which could be attributed to both chemical (i.e. preserved covalent crosslinking by laccases) and physical effects (i.e. higher solid content and enhanced supramolecular interactions upon regeneration). On the contrary, the viscoelastic properties and structural integrity of WAX hydrogels were compromised upon arabinose removal. This suggests that tuning the arabinose content in arabinoxylans isolated from different plant sources directly impacts their biophysical properties in terms of polysaccharide aggregation, influencing the accessibility of the laccases to their ferulic acid substrates for oxidation and crosslinking. Moreover, arabinose removal subsequently hinders the water absorption of the hydrogels (with the concomitant increase in the total solid content) and it also alters the physical interactions and network organisation of the hydrogels upon subsequent freeze drying and regeneration. We propose that

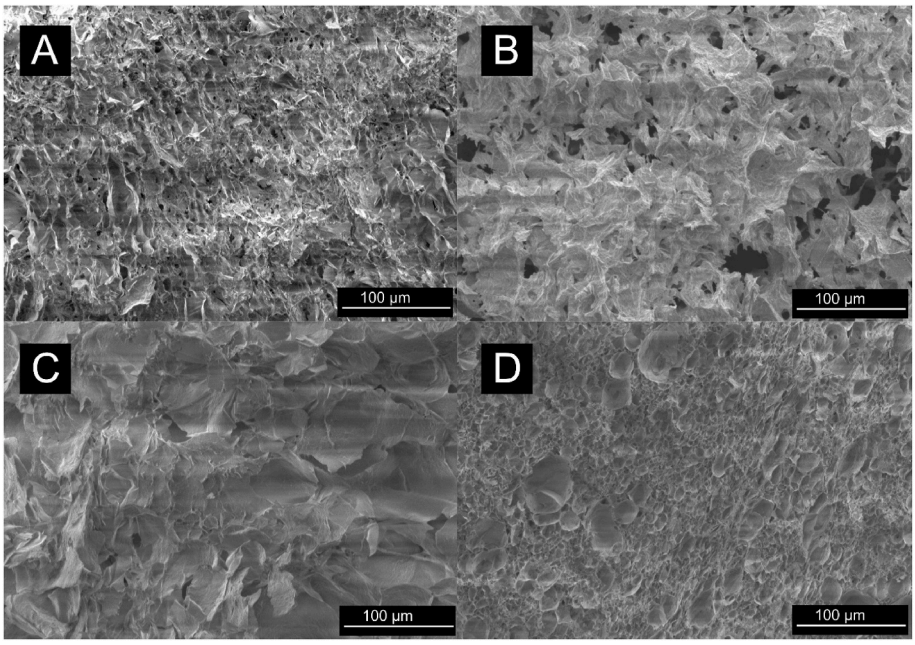

Fig. 6. FE-SEM micrographs showing the morphology of the hydrogels after freeze drying. (A) Laccase-crosslinked WAX hydrogel (WAX L); (B) GH43 and GH62 treated laccase-crosslinked WAX hydrogel (WAX GH43GH62 L); (C) Laccase-crosslinked RAX hydrogel (RAX L); (D) GH43 and GH62 treated laccase-crosslinked RAX hydrogel (RAX GH43GH62 L).

while laccase covalent crosslinking is the main force behind gelation, physical phenomena such as hydration and supramolecular interactions between arabinoxylan chains also influence the overall rheological properties and structure of the hydrogels, sometimes in a diverging way. This study shows how enzyme technology is a selective and effective tool to modulate the functional properties of polysaccharide hydrocolloids for use in food products, where the rheological properties are of great importance for sensory and nutritional properties. The techno-economic potential of this technology for the valorisation of cereal side streams should be the focus of further studies, where aspects like process scalability, enzyme costs, and life cycle assessments should be considered.

CRediT authorship contribution statement

Carl Rämgård: Writing – review & editing, Writing – original draft, Visualization, Validation, Methodology, Investigation, Formal analysis, Data curation. **Marjorie Ladd Parada:** Writing – review & editing, Methodology, Investigation, Formal analysis, Data curation. **Ratchawit Janewithayapun:** Writing – review & editing, Formal analysis, Data curation. **Thu V. Vuong:** Writing – review & editing, Resources. **Emma R. Master:** Writing – review & editing, Resources. **Anna Ström:** Writing – review & editing, Formal analysis. **Lauren S. McKee:** Writing – review & editing, Writing – original draft, Supervision, Conceptualization. **Francisco Vilaplana:** Writing – review & editing, Writing – original draft, Supervision, Project administration, Funding acquisition, Formal analysis, Conceptualization.

Declaration of competing interest

The authors declare the following financial interests/personal relationships which may be considered as potential competing interests: Francisco Vilaplana reports financial support was provided by Swedish Research Council Formas. Carl Rämgård reports equipment, drugs, or supplies was provided by Treesearch. Francisco Vilaplana reports a relationship with Oatly AB that includes: employment. Francisco Vilaplana reports a relationship with Arla Foods amba that includes: board membership. If there are other authors, they declare that they have no known competing financial interests or personal relationships that could have appeared to influence the work reported in this paper.

Acknowledgements

The authors acknowledge the Swedish Research Council Formas for the financial support to this work (Project 2020-01575) and to PLENTY – a Centre for Circular and Symbiotic Food Provisioning (2024-01152). Dr. Reskandi Chastelia Rudjito, Dr. Secil Yilmaz Turan, Dr. Maria Carmen Casado, and Ass. Prof. Amparo Jimenez-Quero are thanked for the previous extraction and characterisation of WAX and RAX substrates. The authors acknowledge Treesearch for the support to access the SAXS facilities at the Department of Material and Surface Design, RISE Research Institute of Sweden (Stockholm, Sweden).

Appendix A. Supplementary data

Supplementary data to this article can be found online at https://doi.org/10.1016/j.foodhyd.2025.112080.

Data availability

Data will be made available on request.

References

Abdulhadi, A., Isabelle, C., Jordane, J., Cédric, P., Joël, S., & Lionel, M. (2014). Laccase-catalysed oxidation of ferulic acid and ethyl ferulate in aqueous medium: A green procedure for the synthesis of new compounds. *Food Chemistry, 145*, 1046–1054.

Adelakun, O. E., Kudanga, T., Parker, A., Green, I. R., le Roes-Hill, M., & Burton, S. G. (2012). Laccase-catalyzed dimerization of ferulic acid amplifies antioxidant activity. *Journal of Molecular Catalysis B: Enzymatic, 74*(1), 29–35.

Aguedo, M., Fougnies, C., Dermience, M., & Richel, A. (2014). Extraction by three processes of arabinoxylans from wheat bran and characterization of the fractions obtained. *Carbohydrate Polymers, 105*, 317–324, 0.

Amritpal, K., Madhav, P. Y., Balwinder, S., Seerat, B., Stefanie, S., & Narpinder, S. (2019). Isolation and characterization of arabinoxylans from wheat bran and study of their contribution to wheat flour dough rheology. *Carbohydrate Polymers, 221*, 166–173.

Arens, U. (2015). 7 - Authorised EU health claim for rye fibre. In M. J. Sadler (Ed.), *Foods, nutrients and food ingredients with authorised EU health claims* (Vol. 2, pp. 129–137). Oxford: Woodhead Publishing.

Aura, A.-M. (2014). Chapter 7 - Phenolic acids in rye. In K. Poutanen, & P. Åman (Eds.), *Rye and health* (pp. 109–119). AACC International Press.
Bakó, I., Pusztai, L., & Temleitner, L. (2017). Decreasing temperature enhances the formation of sixfold hydrogen bonded rings in water-rich water-methanol mixtures. *Scientific Reports, 7*(1), 1073.
Birdsong, B., Capezza, A. J., Nejati, M., Bjurström, A., Li, Y., Jimenez Quero, A., & Olsson, R. (2024). Silicon oxide nanofibers using fungi mycelium as template material/from water purification to space insulation. *RSC Applied Interfaces*.
Broekaert, W. F., Cloetens, L., Courtin, C. M., Delaedt, Y., Delcour, J. A., Ollevier, F., Rutgeerts, P., & Verbeke, K. (2010). Tolerance of arabinoxylan-oligosaccharides and their prebiotic activity in healthy subjects: A randomised, placebo-controlled cross-over study. *British Journal of Nutrition, 103*(5), 703–713.
Brummer, Y., Defelice, C., Wu, Y., Kwong, M., Wood, P. J., & Tosh, S. M. (2014). Textural and rheological properties of oat beta-glucan gels with varying molecular weight composition. *Journal of Agricultural and Food Chemistry, 62*(14), 3160–3167.
Carunchio, F., Crescenzi, C., Girelli, A. M., Messina, A., & Tarola, A. M. (2001). Oxidation of ferulic acid by laccase: Identification of the products and inhibitory effects of some dipeptides. *Talanta, 55*(1), 189–200.
Carvajal-Millan, E., Landillon, V., Morel, M.-H., Rouau, X., Doublier, J.-L., & Micard, V. (2005). Arabinoxylan gels: Impact of the feruloylation degree on their structure and properties. *Biomacromolecules, 6*(1), 309–317.
Cui, S. W., Wu, Y., & Ding, H. (2013). 5 - The range of dietary fibre ingredients and a comparison of their technical functionality. In J. A. Delcour, & K. Poutanen (Eds.), *Fibre-rich and wholegrain foods* (pp. 96–119). Woodhead Publishing.
De Ruiter, G. A., Schols, H. A., Voragen, A. G. J., & Rombouts, F. M. (1992). Carbohydrate analysis of water-soluble uronic acid-containing polysaccharides with high-performance anion-exchange chromatography using methanolysis combined with TFA hydrolysis is superior to four other methods. *Analytical Biochemistry, 207*(1), 176–185.
EUROSTAT. (2021). *Food waste and food waste prevention by NACE rev. 2 activity - Tonnes of fresh mass* (2023 ed.).
Fao, F. (2014). Food wastage footprint full-cost accounting. *Food Wastage Footprint*.
Fry, S. C., Willis, S. C., & Paterson, A. E. (2000). Intraprotoplasmic and wall-localised formation of arabinoxylan-bound diferulates and larger ferulate coupling-products in maize cell-suspension cultures. *Planta, 211*, 679–692.
Garcia-Conesa, M. T., Plumb, G. W., Waldron, K. W., Ralph, J., & Williamson, G. (1997). Ferulic acid dehydrodimers from wheat bran: Isolation, purification and antioxidant properties of 8-0-4-diferulic acid. *Redox Report, 3*(5–6), 319–323.
Geissmann, T., & Neukom, H. (1973). Note of ferulic acid as a constituent of the water-insoluble pentosans of wheat flour. *Cereal Chemistry, 50*, 414–416.
Gustavsson, J., Cederberg, C., Sonesson, U., Van Otterdijk, R., & Meybeck, A. (2011). *Global food losses and food waste*. FAO Rome.
Hatfield, R. D., Ralph, J., & Grabber, J. H. (1999). Cell wall cross-linking by ferulates and diferulates in grasses. *Journal of the Science of Food and Agriculture, 79*(3), 403–407.
Höije, A., Stememalm, E., Heikkinen, S., Tenkanen, M., & Gatenholm, P. (2008). Material properties of films from enzymatically tailored arabinoxylans. *Biomacromolecules, 9*(7), 2042–2047.
Ikehata, K., Buchanan, I. D., & Smith, D. W. (2004). Recent developments in the production of extracellular fungal peroxidases and laccases for waste treatment. *Journal of Environmental Engineering and Science, 3*(1), 1–19.
Janewithayapun, R., Cousin, F., de Moura Pereira, P. F., Herranz-Trillo, F., Terry, A. E., Pedersen, J. S., Quero, A. J., & Ström, A. (2025). Correlation between arabinose content and the conformation of arabinoxylan in water dispersions. *Carbohydrate Polymers*, Article 124082.
Johnson, A. M., Karaaslan, M. A., Cho, M., Ogawa, Y., & Renneckar, S. (2023). Exploring the impact of water on the morphology and crystallinity of xylan hydrate nanotiles. *Carbohydrate Polymers, 319*, Article 121165.
Kishani, S., Escalante, A., Toriz, G., Vilaplana, F., Gatenholm, P., Hansson, P., & Wagberg, L. (2019). Experimental and theoretical evaluation of the solubility/insolubility of Spruce Xylan (Arabino glucuronoxylan). *Biomacromolecules, 20*(3), 1263–1270.
Kudanga, T., Nyanhongo, G. S., Guebitz, G. M., & Burton, S. (2011). Potential applications of laccase-mediated coupling and grafting reactions: A review. *Enzyme and Microbial Technology, 48*(3), 195–208.
Liu, J., Sun, D., Zhu, J., Liu, C., & Liu, W. (2021). Carbohydrate-binding modules targeting branched polysaccharides: Overcoming side-chain recalcitrance in a non-catalytic approach. *Bioresources and Bioprocessing, 8*(1), 28.
Luc, S., Pierre-Etienne, S., Gérard, B., Gilles, C., & Fabienne, G. (2007). Wheat arabinoxylans: Exploiting variation in amount and composition to develop enhanced varieties. *Journal of Cereal Science, 46*(3), 261–281.
Lundin, C. D., Zhou, G., & Prager, M. (1998). Cryo-cracking: A technique for creep damage assessment in high temperature components. *Materials at High Temperatures, 15*(3–4), 167–173.
Marquez-Escalante, J. A., Carvajal-Millan, E., Yadav, M. P., Kale, M., Rascon-Chu, A., Gardea, A. A., Valenzuela-Soto, E. M., Lopez-Franco, Y. L., Lizardi-Mendoza, J., & Faulds, C. B. (2018). Rheology and microstructure of gels based on wheat arabinoxylans enzymatically modified in arabinose to xylose ratio. *Journal of the Science of Food and Agriculture, 98*(3), 914–922.
McGregor, N. G. S., Turkenburg, J. P., Mørkeberg Krogh, K. B. R., Nielsen, J. E., Artola, M., Stubbs, K. A., Overkleeft, H. S., & Davies, G. J. (2020). Structure of a GH51 α-L-arabinofuranosidase from Meripilus giganteus: Conserved substrate recognition from bacteria to fungi. *Acta Crystallogr D Struct Biol, 76*(Pt 11), 1124–1133.
McKee, L. S., Peña, M. J., Rogowski, A., Jackson, A., Lewis, R. J., & York, W. S. (2012). Introducing endo-xylanase activity into an exo-acting arabinofuranosidase that targets side chains. *Proceedings of the National Academy of Sciences of the United States of America, 109*.
Mendis, M., & Simsek, S. (2014). Arabinoxylans and human health. *Food Hydrocolloids, 42*, 239–243.
Menzel, C., González-Martínez, C., Chiralt, A., & Vilaplana, F. (2019). Antioxidant starch films containing sunflower hull extracts. *Carbohydrate Polymers, 214*, 142–151.
Neves, M. A.d., Kimura, T., Shimizu, N., & Shiiba, K. (2006). Production of alcohol by simultaneous saccharification and fermentation of low-grade wheat flour. *Brazilian Archives of Biology and Technology, 49*, 481–490.
Nieduszynski, I. A., & Marchessault, R. H. (1972). Structure of β,D(1–>4′)-xylan hydrate. *Biopolymers, 11*(7), 1335–1344.
Nyström, L., Lampi, A.-M., Andersson, A. A. M., Kamal-Eldin, A., Gebruers, K., Courtin, C. M., Delcour, J. A., Li, L., Ward, J. L., Fraś, A., Boros, D., Rakszegi, M., Bedő, Z., Shewry, P. R., & Piironen, V. (2008). Phytochemicals and dietary fiber components in rye varieties in the HEALTHGRAIN diversity screen. *Journal of Agricultural and Food Chemistry, 56*(21), 9758–9766.
Oluyemisi, E. A., Tukayi, K., Ayesha, P., Ivan, R. G., Marilize, & Stephanie, G. B. (2012). Laccase-catalyzed dimerization of ferulic acid amplifies antioxidant activity. *Journal of Molecular Catalysis B: Enzymatic, 74*(1), 29–35.
Rahman, A., Ulven, C. A., Durant, C., Johnson, M. A., Fehrenbach, J., & Hossain, K. G. (2017). Selection, pretreatment, and use of wheat bran for making thermoplastic composite. In *2017 ASABE annual international meeting* (p. 1). St. Joseph, MI: ASABE.
Rosicka-Kaczmarek, J., Komisarczyk, A., Nebesny, E., & Makowski, B. (2016). The influence of arabinoxylans on the quality of grain industry products. *European Food Research and Technology, 242*(3), 295–303.
Rudjito, R. C., Jiménez-Quero, A., Hamzaoui, M., Kohnen, S., & Vilaplana, F. (2020). Tuning the molar mass and substitution pattern of complex xylans from corn fibre using subcritical water extraction. *Green Chemistry, 22*(23), 8337–8352.
Rudjito, R. C., Jiménez-Quero, A., Muñoz, M. D. C. C., Kuil, T., Olsson, L., Stringer, M. A., Krogh, K. B. R. M., Eklöf, J., & Vilaplana, F. (2023). Arabinoxylan source and xylanase specificity influence the production of oligosaccharides with prebiotic potential. *Carbohydrate Polymers, 320*, Article 121233.
Ruthes, A. C., Martínez-Abad, A., Tan, H.-T., Bulone, V., & Vilaplana, F. (2017). Sequential fractionation of feruloylated hemicelluloses and oligosaccharides from wheat bran using subcritical water and xylanolytic enzymes. *Green Chemistry, 19*(8), 1919–1931.
Ruthes, A. C., Rudjito, R. C., Rencoret, J., Gutiérrez, A., del Río, J. C., Jiménez-Quero, A., & Vilaplana, F. (2020). Comparative recalcitrance and extractability of cell Wall polysaccharides from cereal (Wheat, rye, and barley) brans using subcritical water. *ACS Sustainable Chemistry & Engineering, 8*(18), 7192–7204.
Selig, M. J., Thygesen, L. G., Felby, C., & Master, E. R. (2015). Debranching of soluble wheat arabinoxylan dramatically enhances recalcitrant binding to cellulose. *Biotechnology Letters, 37*(3), 633–641.
Sørensen, H. R., Jørgensen, C. T., Hansen, C. H., Jørgensen, C. I., Pedersen, S., & Meyer, A. S. (2006). A novel GH43 alpha-L-arabinofuranosidase from Humicola insolens: Mode of action and synergy with GH51 alpha-L-arabinofuranosidases on wheat arabinoxylan. *Applied Microbiology and Biotechnology, 73*(4), 850–861.
Stevenson, L., Phillips, F., O'Sullivan, K., & Walton, J. (2012). Wheat bran: Its composition and benefits to health, a European perspective. *International Journal of Food Sciences & Nutrition, 63*(8), 1001–1013.
Vansteenkiste, E., Babot, C., Rouau, X., & Micard, V. (2004). Oxidative gelation of feruloylated arabinoxylan as affected by protein. Influence on protein enzymatic hydrolysis. *Food Hydrocolloids, 18*(4), 557–564.
Viëtor, R. J., Kormelink, F. J. M., Angelino, S. A. G. F., & Voragen, A. G. J. (1994). Substitution patterns of water-unextractable arabinoxylans from barley and malt. *Carbohydrate Polymers, 24*(2), 113–118.
Vuong, T. V., Aghajohari, M., Feng, X., Woodstock, A. K., Nambiar, D. M., Sleiman, Z. C., Urbanowicz, B. R., & Master, E. R. (2024). Enzymatic routes to designer hemicelluloses for use in biobased materials. *JACS Au, 4*(11), 4044–4065.
Vuong, T. V., & Master, E. R. (2022). Enzymatic upgrading of heteroxylans for added-value chemicals and polymers. *Current Opinion in Biotechnology, 73*, 51–60.
Wang, W., Mai-Gisondi, G., Stogios, P. J., Kaur, A., Xu, X., Cui, H., Turunen, O., Savchenko, A., & Master, E. R. (2014). Elucidation of the molecular basis for arabinoxylan-debranching activity of a thermostable family GH62 α-l-arabinofuranosidase from Streptomyces thermoviolaceus. *Applied and Environmental Microbiology, 80*(17), 5317–5329.
Watkins, A. M., Bonneau, R., & Arora, P. S. (2016). Side-chain conformational preferences govern protein–protein interactions. *Journal of the American Chemical Society, 138*(33), 10386–10389.
Yilmaz-Turan, S., Jiménez-Quero, A., Menzel, C., de Carvalho, D. M., Lindström, M. E., Sevastyanova, O., Moriana, R., & Vilaplana, F. (2020). Bio-based films from wheat bran feruloylated arabinoxylan: Effect of extraction technique, acetylation and feruloylation. *Carbohydrate Polymers, 250*, Article 116916.
Yilmaz-Turan, S., Jiménez-Quero, A., Moriana, R., Arte, E., Katina, K., & Vilaplana, F. (2020). Cascade extraction of proteins and feruloylated arabinoxylans from wheat bran. *Food Chemistry, 333*, Article 127491.
Yilmaz-Turan, S., Lopez-Sanchez, P., Jiménez-Quero, A., Plivelic, T. S., & Vilaplana, F. (2022). Revealing the mechanisms of hydrogel formation by laccase crosslinking and regeneration of feruloylated arabinoxylan from wheat bran. *Food Hydrocolloids, 128*, Article 107575.
Yu, Y., Tyrikos-Ergas, T., Zhu, Y., Fittolani, G., Bordoni, V., Singhal, A., Fair, R. J., Grafmüller, A., Seeberger, P. H., & Delbianco, M. (2019). Systematic hydrogen-bond

manipulations to establish polysaccharide structure–property correlations. *Angewandte Chemie International Edition, 58*(37), 13127–13132.
Zhang, X., Chen, T., Lim, J., Gu, F., Fang, F., Cheng, L., Campanella, O. H., & Hamaker, B. R. (2019). Acid gelation of soluble laccase-crosslinked corn bran arabinoxylan and possible gel formation mechanism. *Food Hydrocolloids, 92*, 1–9.
Zheng, J., Guo, N., Huang, Y., Guo, X., & Wagner, A. (2024). High temperature delays and low temperature accelerates evolution of a new protein phenotype. *Nature Communications, 15*(1), 2495.